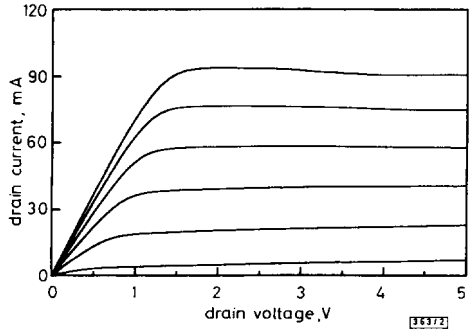

Fig. 2 *Typical DC current-voltage characteristics of high-low doped GaAs power MESFET with gate width of 300μm*

Top curve corresponds to V_{gs} = 0.5V and ΔV_{gs} = 0.5V

the typical DC current-voltage characteristics of the FET. The gate-to-drain breakdown voltage, measured at a gate current density of 1mA/mm, was 28V. The maximum drain current density I_{max}, defined as the drain current density measured at V_{gs} = 0.5V, was 310mA/mm. Low output conductance and constant transconductance with gate voltage are observed. A uniform transconductance (g_m) of ~112mS/mm, ranging from V_g = -1.8V to 0.5V for the FET with a gate width of 300μm, is obtained as shown in Fig. 3. The power characteristics of the FETs were measured at 900MHz with a drain bias of 3.3V by the load-pull method using an automated tuner system. The device was operated under class AB condition with a bias current of 0.3A, corresponding to 10% of I_{max}. An output power of 30.9dBm and PAE of 65% were obtained for an input power of 20dBm. The linear power gain was measured to be 16.9dB. When the drain bias increases to 3.5V, an output power of 31.5dBm with PAE of 65% at an input power of 20dBm, and linear power gain of 16.9dB, were obtained. The performance characteristics are similar to the previous results [4], while the linear power gain is much higher than that of 12dB [4]. It is believed that the power MESFET developed in this work is adequate for digital communications because the high power gain could cause high PAE in the linear region of the output power. The devices were also tested at a drain bias of 3.0V. The output power was 30.3dBm with a PAE of 65% at an input power of 20dBm.

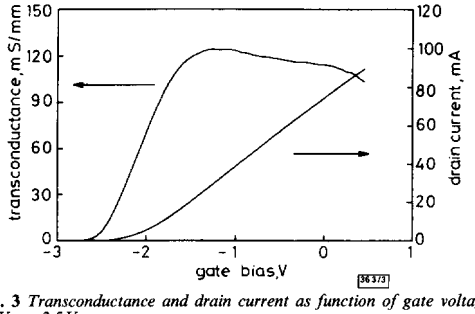

Fig. 3 *Transconductance and drain current as function of gate voltage at V_{ds} = 2.5V*

Gate width is 300μm

State-of-the-art GaAs power MESFETs operating at 3.3V have been developed using the high-low doped channel structure. The power MESFETs developed in this work are expected to be used as a power amplifying device in hand-held telephones for the next generation.

Acknowledgment: This work was financially supported by the Ministry of Communications in Korea.

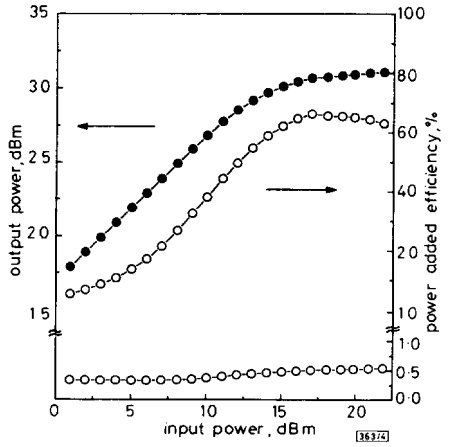

Fig. 4 *Output power, power-added efficiency, and drain current as function of input power for GaAs power MESFET with gate width of 12mm*

Data were taken at 900MHz at drain bias of 3.3V

7 March 1994
Electronics Letters Online No: 19940477

J.-L. Lee, H. Kim, J.K. Mun , O. Kwon, J.J. Lee, H.-M. Park and S.-C. Park (*Semiconductor Division, Electronics and Telecommunications Research Institute, Yusong, PO Box 106, Taejon, Korea*)

References

1 NGO, D., BECKWITH, B., O'NEIL, P., and CAMILLERI, N.: 'Low voltage GaAs power amplifiers for personal communications at 1.9GHz'. *IEEE MTT-S Dig.*, June 1993, pp. 1461–1464

2 IWATA, N., INOSAKO, K., and KUZUHARA, M.: '3V operation L-band power double-doped heterojunction FETs', *IEEE MTT-S Dig.*, June 1993, pp. 1465–1468

3 MURAI, S., SAWAI, T., YAMAGUCHI, T., and HARADA, Y.: 'A high power-added efficiency GaAs power MESFET and MMIC operating at a very low drain bias for use in personal handy phones', *IEICE Trans.Electron*, 1993, **E76-C**, pp. 901–907

4 MAEDA, M., NISHIJIMA, M., TAKEHARA, H., ADACHI, C., FUJIMOTO, H., OTA, Y., and ISHIKAWA, O.: 'A 3.5V, 1.3W GaAs power multi chip IC for cellular phone'. GaAs IC Symp. Tech. Dig., October 1993, pp. 53–56

5 LEE, J.-L., KIM, D., MAENG, S.J., PARK, H.H., KANG, J.Y., and LEE, Y.T.: 'Improvement of breakdown characteristics of GaAs power FET using $(NH_4)_2S_x$ treatment', *J. Appl. Phys.*, 1993, **73**, pp. 3539–3524

Defuzzification method for multishaped output fuzzy sets

S.H. Jung, K.H. Cho, T.G. Kim and K.H. Park

Indexing terms: Fuzzy control, Control theory

A defuzzification method is an important performance factor in fuzzy logic controllers (FLCs). When an FLC uses multishaped output fuzzy sets, existing defuzzification methods have the fat shape dominance phenomenon. The authors propose a new defuzzification method for multishaped output fuzzy sets. The method takes the degree of certainty on the fired level into account in the defuzzification process. Simulation experiments with a nonlinear plant show that an FLC employing the proposed defuzzification method is more stable and robust than existing FLCs.

Introduction: In a fuzzy logic controller (FLC), the final control outputs depend not only on the rules used but on the inference and defuzzification method [1]. Also, the shapes of output fuzzy

sets have a great effect on the output of defuzzification. However, when an FLC uses multishaped output fuzzy sets, the problem of the fat shape dominance phenomenon may arise [3].

Yu *et al.* [3] proposed an inference method, and Hellendoorn *et al.* [2] introduce a new defuzzification method for multishaped output fuzzy sets. The Hellendoorn method depends only on the area of the clipped output fuzzy set regardless of the degree of certainty on the fired level.

We develop a new defuzzification method which takes into account the degree of certainty on the fired level, namely, α-cut. The Hellendoorn method is a special case of our defuzzification method. This fact indicates that our method can be viewed as an extension of his method. The simulation results show that our defuzzification method is more stable and robust than the Hellendoorn method.

Fat shape dominance phenomenon: The problem of the fat shape dominance phenomenon [3] is summarised as: when an FLC uses output fuzzy sets which have different or asymmetrical shapes, the final FLC outputs are mainly influenced by the fat shape output membership element even though the membership is fuzzier than the slim shape element.

If the rules of an FLC are inconsistent, then this phenomenon becomes more severe.

New defuzzification method: First, we define the measure of certainty which is used as a basis of our defuzzification method.

(i) Definition 1: Measure of certainty of α-cut: Let $X \subset R^1$ be the universe of discourse and $x \in X$. Let F_X be a family of fuzzy sets on X and $A \in F_X$, and let $w_A(\alpha)$ be the support length of α-cut; the measure of certainty of α-cut is then defined as

$$m_c(\alpha) = \frac{\alpha}{w_A(\alpha)} = \frac{\alpha}{\mu_A^{-1}(\alpha)_{max} - \mu_A^{-1}(\alpha)_{min} + 1} \quad (1)$$

where $\mu_A^{-1}(\alpha)$ is the inverse membership function of A.

Hellendoorn *et al.* [2] propose a defuzzification method to solve the fat shape dominance phenomenon for multishaped output fuzzy sets. Eqn. 2 shows his defuzzification method:

$$u^* = \frac{\sum_{i=1}^{n} \frac{s_{im}\alpha_i^2}{area(S_i)}}{\sum_{i=1}^{n} \frac{\alpha_i^2}{area(S_i)}} \quad (2)$$

where α_i is the value with which the rule R_i fires, $s_{im} = \mu^{-1}(1)$ and S_i is the clipped output of the fired rule. His method does not consider the degree of certainty of output fuzzy sets on the level of α-cut.

On the basis of the discussion, we propose a new defuzzification method which depends on the degree of certainty on the level of α-cut. We call the method the level grading method (LGM). If an FLC uses n output fuzzy sets, then the LGM is given as follows:

$$u^* = \frac{\sum_{i=1}^{n} s_{im} m_c(\alpha_i)}{\sum_{i=1}^{n} m_c(\alpha_i)} = \frac{\sum_{i=1}^{n} \frac{s_{im}\alpha_i}{w_{A_i}(\alpha_i)}}{\sum_{i=1}^{n} \frac{\alpha_i}{w_{A_i}(\alpha_i)}} \quad (3)$$

where α_i is the value with which the rule R_i fires, $s_{im} = \mu^{-1}(1)$, and $w_A(\alpha_i)$ is the support length of α-cut.

Fig. 1 shows the comparison of two methods, i.e., QM and LGM. As we intuitively expect, the output of defuzzification in Fig. 1*b* should be near the left membership function because the degree of certainty of the left membership function on the fired level is larger than that of Fig. 1*a*.

As a special case, if all output fuzzy sets have rectangular shapes, then the support length on the all level of α-cut becomes constant. Finally our method becomes the same as the QM as shown in eqn. 4.

$$u^* = \frac{\sum_{i=1}^{n} \frac{s_{im}\alpha_i}{w_i}}{\sum_{i=1}^{n} \frac{\alpha_i}{w_i}} = \frac{\sum_{i=1}^{n} \frac{s_{im}\alpha_i^2}{w_i\alpha_i}}{\sum_{i=1}^{n} \frac{\alpha_i^2}{w_i\alpha_i}} = \frac{\sum_{i=1}^{n} \frac{s_{im}\alpha_i^2}{area(S_i)}}{\sum_{i=1}^{n} \frac{\alpha_i^2}{area(S_i)}} \quad (4)$$

where w_i is the support length of the fuzzy set. This is due to the fact that in the QM the certainties of a fuzzy set on the all levels of α-cut are equal. This fact indicates that our method is more general and reasonable than the QM.

Simulation: In our simulation, two membership functions corresponding to the NS and PS terms are in fat-shape form, and three membership functions corresponding to NZ, ZO, and PZ terms are in slim-shape form. We use inconsistent rules as shown in Table 1. The nonlinear plant model used in the simulation is given by a difference equation form, $y(k+1) = y(k)/(1 + y^2(k))u(k) + u(k)$. Using the inconsistent rules, simulation experiments have been carried out for two cases: Mamdani-QM, and Mamdani-LGM. The simulation result shows that the LGM defuzzification reduces the steady state error and settling time; and eliminates the chattering effect more successfully than the QM as shown in Fig. 2.

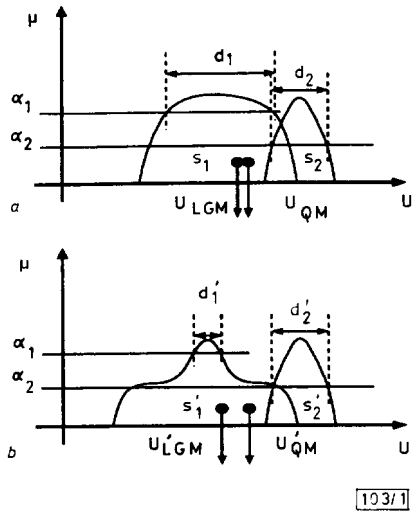

Fig. 1 Comparison between LGM and QM

Conditions:
$s_1 = s_1'$
$s_2 = s_2'$
$d_1 \neq d_1'$
$d_1 = d_1'$
Conculsions:
$U_{QM} = U'_{QM}$
$U_{LGM} \neq U'_{LGM}$

Table 1: Inconsistent rule table

e/ce	nb	ns	nz	zo	pz	ps	pb
nb	nb	nb	nb	nb	ns	ns/nz	zo
ns	nb	nb	nb	ns	ns/nz	zo	pz/ps
nz	nb	nb	ns	ns/nz	zo	pz/ps	ps
zo	nb	ns	ns/nz	zo	pz/ps	ps	pb
pz	ns	ns/nz	zo	pz/ps	ps	pb	pb
ps	ns/nz	zo	pz/ps	ps	pb	pb	pb
pb	zo	pz/ps	ps	pb	pb	pb	pb

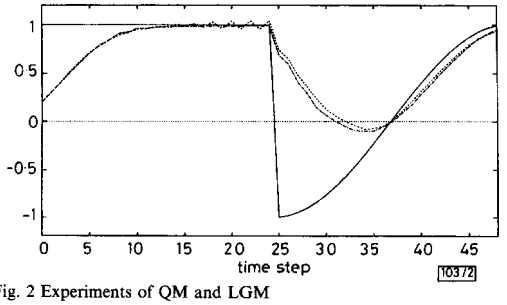

Fig. 2 Experiments of QM and LGM

——— Set points
· · · · · Mam-QM
– · – · Mam-LGM

Conclusion: A new defuzzification method termed LGM was proposed for an FLC with multishaped or asymmetrical output fuzzy sets. An FLC using our defuzzification method was constructed and applied to the simulation of nonlinear plant control using typical inconsistent rules. Simulation results showed that our defuzzification method was more stable and robust than QM in the presence of inconsistent rules.

14 February 1994
Electronics Letters Online No: 19940468

S. H. Jung, K. H. Cho, T. G. Kim and K. H. Park (*Department of Electrical Engineering, Korea Advanced Institute of Science and Technology, 373-1, Kusong-dong, Yusong-gu, Taejon 305-701, Korea*)

References

1 W. PEDRYCZ: 'Fuzzy control and fuzzy systems' (Research Study Press, 1989)
2 HELLENDOORN, H., and THOMAS, C.: 'Defuzzification in fuzzy controllers', *J. Intelligent and Fuzzy Systems*, 1993, **1**, pp. 109–123
3 YU, W., and BIEN, Z.: 'Design of fuzzy logic controller with inconsistent rule base'. 5th IFSA World Congress, 1993, **2**, pp. 1370–1373

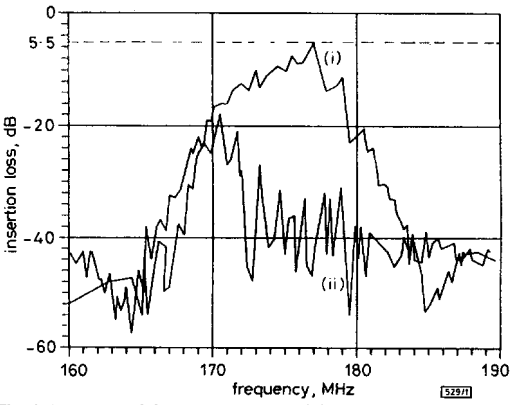

Fig. 1 *Experimental frequency response of down and up chirp filters in 50Ω tract without matching elements*

(i) down chirp filters
(ii) up chirp filters

Unidirectionality in dispersive SAW transducers

S.A. Zhgoon, V.A. Kalinin, S.A. Orlov and B.N. Dunaev

Indexing terms: Surface acoustic waves, Transducers, Filters

Low loss SAW filters can be built making use of unidirectionality and selfmatching of dispersive transducers. The origin of unidirectionality lies in internal reflections between electrodes. The calculated loss level may be as low as 0.08dB in down chirp double dispersive IDT filters.

It is well known that dispersive filters with in-line IDTs, especially for up chirps, do not usually lead to a high quality frequency response. The classic explanation to account for the response distortion is based on bulk wave generation [1]. Slanted double dispersive transducers are strongly recommended for overcoming this problem. Tankrell and Holland [2] observed that the triple transit signal in filters with chirp IDTs is lower than in filters with uniform IDTs. They attributed this fact to unidirectionality arising from apodisation of chirp IDT. They also mentioned internal reflections and regeneration as factors affecting the frequency response of a filter. A nondispersive unidirectional IDT based on local reflections is described in [3].

We have discovered in experiments with in-line double dispersive IDTs that the insertion loss for down chirps without external matching to a 50Ω circuit may reach values lower than 6dB, implying the presence of unidirectionality effects.

In our experiments we have used both down chirps and up chirps. The transducers have been designed for the frequency band 173–183MHz with $T = 2\mu s$ and $BT = 20$. The number, N, of electrodes is 712, with an electrode separation of 5.6μm. The position of the nth electrode is given by $x(n)$, where

$$x(n) = 798.2[(29929 + 5n)^{1/2} - 173] \quad [\mu m]$$

The substrate is $Y + 128°$ rotated cut $LiNbO_3$ with dimensions of $18 \times 2mm^2$. The transducer aperture $W = 83\mu m$; it is assumed that lateral diffraction is largely suppressed by the waveguiding action of the transducer.

The experimental insertion loss of the down chirp and of the up chirp filters is shown in Fig. 1, and the transducer impedance in Fig. 2. The latter shows that the transducer impedance is very close to satisfying a selfmatching condition. However the unexpected low loss of a down chirp filter cannot be understood on the basis of selfmatching only. It has encouraged us to produce more accurate numerical calculations of the transducers with the use of

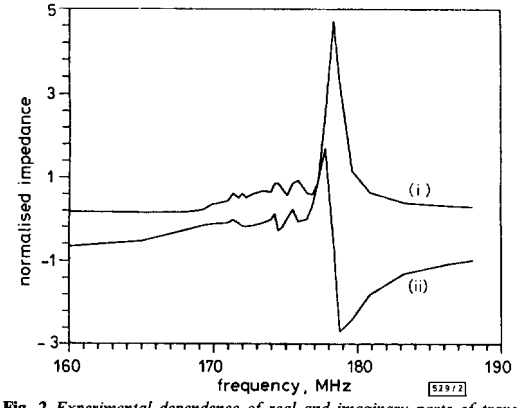

Fig. 2 *Experimental dependence of real and imaginary parts of transducer impedance*

Impedance values are normalised by 50Ω
(i) real part
(ii) imaginary part

the equivalent circuit model [4], taking internal reflections and regeneration of SAWs into account, but excluding bulk wave generation and diffraction effects.

Clear evidence of unidirectionality can be observed in Fig. 3. The calculated minimum loss level is as low as 0.08dB for a down chirp without including any external matching. The calculated impedance characteristic (Fig. 4) confirms the selfmatching property of the transducer.

To understand the nature of the unidirectionality we have calculated the response of up and down chirp filters, for a quartz substrate and for very thin electrodes. This is equivalent to exclusion from the model of internal reflection and significant reduction of regeneration. In this case both curves have become almost identical, and show the classic Fresnel ripples. When we now include mass loading in this calculation by increasing the thickness of the electrodes, we see a significant degree of unidirectionality. Using the same program for $LiNbO_3$, with compensation for internal reflections, but still allowing for regeneration, the ripple swing is higher than for quartz, but the unidirectionality is not encountered. The reflection compensation is achieved in this case by excluding the characteristic impedance mismatch between active and passive sections of the IDT from the model [4].

From these results we may conclude that internal reflections between electrodes in the dominant origin of the unidirectionality of these transducers, while other effects, such as regeneration, bulk move generation etc. play only a secondary role. The effect is